JCB Article

The intraflagellar transport protein, IFT88, is essential for vertebrate photoreceptor assembly and maintenance

Gregory J. Pazour,[1] Sheila A. Baker,[4] James A. Deane,[2] Douglas G. Cole,[3] Bethany L. Dickert,[1] Joel L. Rosenbaum,[2] George B. Witman,[1] and Joseph C. Besharse[4]

[1]Department of Cell Biology, University of Massachusetts Medical School, Worcester, MA 01655
[2]Department of Molecular, Cellular, and Developmental Biology, Yale University, New Haven, CT 06520
[3]Department of Microbiology, Molecular Biology, and Biochemistry, University of Idaho, Moscow, ID 83844
[4]Department of Cell Biology, Neurobiology, and Anatomy, Medical College of Wisconsin, Milwaukee, WI 53226

Approximately 10% of the photoreceptor outer segment (OS) is turned over each day, requiring large amounts of lipid and protein to be moved from the inner segment to the OS. Defects in intraphotoreceptor transport can lead to retinal degeneration and blindness. The transport mechanisms are unknown, but because the OS is a modified cilium, intraflagellar transport (IFT) is a candidate mechanism. IFT involves movement of large protein complexes along ciliary microtubules and is required for assembly and maintenance of cilia. We show that IFT particle proteins are localized to photoreceptor connecting cilia. We further find that mice with a mutation in the IFT particle protein gene, Tg737/IFT88, have abnormal OS development and retinal degeneration. Thus, IFT is important for assembly and maintenance of the vertebrate OS.

Introduction

Intraflagellar transport (IFT)* (Kozminski et al., 1993) is essential for the assembly and maintenance of sensory cilia in *Caenorhabditis*, motile cilia in sea urchins and *Chlamydomonas*, and primary cilia in mice, and is likely to be important in all cilia. During IFT, kinesin-II transports a large protein complex from the cell body to the tip of the flagellum (Morris and Scholey, 1997; Piperno and Mead, 1997; Cole et al., 1998; Orozco et al., 1999; Signor et al., 1999b). These particles are then returned to the cell body by the DHC1b/DHC2 isoform of cytoplasmic dynein (Pazour et al., 1998, 1999; Porter et al., 1999; Signor et al., 1999a). IFT particles in *Chlamydomonas* are composed of at least 17 proteins and are thought to carry components needed to build and maintain the ciliary axoneme and membrane (Piperno and Mead, 1997; Cole et al., 1998). The functions of individual IFT particle proteins are not known, but their sequences are conserved among green algae, nematodes, and vertebrates (Cole et al., 1998). Mutations in genes encoding IFT particle proteins prevent ciliary assembly in *Chlamydomonas*, *Caenorhabditis*, and mice (Cole et al., 1998; Murcia et al., 2000; Pazour et al., 2000).

Vertebrate photoreceptors are polarized sensory neurons consisting of a photosensitive outer segment (OS) that develops from a nonmotile primary cilium by movement of membrane and phototransduction proteins, such as opsin, into the cilium (Besharse and Horst, 1990). The cilium remains in mature photoreceptors as the sole connecting link between the inner segment (IS) and OS and is presumably the major transport corridor. Mature photoreceptors continue to require transport from the IS to the OS to replace components of the OS that are turned over each day (Young, 1967). It has been estimated that normal turnover in each mammalian OS requires delivery of as many as 2,000 photopigment molecules per minute throughout the life of the cell (Besharse and Horst, 1990). In the larger photoreceptors of amphibians, this rate must be increased by more than an order of magnitude (Besharse and Horst, 1990). In addition to photopigment molecules, phototransduction proteins (Philp et al., 1987; Whelan and McGinnis, 1988) and phos-

Address correspondence to Dr. Joseph C. Besharse, Department of Cell Biology, Neurobiology, and Anatomy, Medical College of Wisconsin, 8701 Watertown Plank Rd., Milwaukee, WI 53226. Tel.: (414) 456-8260. Fax: (414) 456-6517. E-mail: jbeshars@mcw.edu

*Abbreviations used in this paper: DEPC, detergent-extracted photoreceptor cytoskeleton; IFT, intraflagellar transport; IS, inner segment; OS, outer segment; ONL, outer nuclear layer; p, postnatal day; RP, retinitis pigmentosa; RPE, retinal pigment epithelium.

Key words: rods and cones; retinitis pigmentosa; blindness; primary cilia; orpk

pholipid components of the discs (Anderson et al., 1980) also turn over rapidly. Although disruption of intersegmental transport results in photoreceptor degeneration and blindness (Li et al., 1996; Hagstrom et al., 1999; Clarke et al., 2000), the transport mechanisms have not been identified.

IFT has been proposed as a connecting cilium transport mechanism (Rosenbaum et al., 1999). In support of this idea, Marszalek et al. (2000) showed that a conditional knockout of KIF3A, which is a subunit of the anterograde IFT motor, leads to retinal degeneration. However, KIF3A-containing motors are believed to be involved in other cellular processes, including neuronal transport, melanosome movement, and secretory pathway transport (Marszalek and Goldstein, 2000). To more directly test the role of IFT in connecting cilium transport, we here investigate the distribution of IFT particle proteins in vertebrate retinas, and examine the effect of a mutation in an IFT particle subunit gene on the mouse retina. We show that mouse homologues of four *Chlamydomonas* IFT particle proteins are localized to the connecting cilium, and mice with a mutation in the Tg737/IFT88 subunit of the IFT particle form abnormal OSs followed by progressive photoreceptor degeneration. These data strongly suggest that IFT is an important transport mechanism in vertebrate photoreceptors and raise the possibility that defects in IFT may cause some forms of human blindness.

Results

Vertebrate IFT particle proteins

The *Chlamydomonas* IFT particle is composed of ~17 proteins. We have used peptide sequence obtained from purified particle proteins to clone and sequence the *Chlamydomonas* genes, which were then used to identify mammalian homologues in Genbank/EMBL/DDBJ. Mammalian homologues of IFT88, IFT57, IFT52, and IFT20 were chosen for further study in this work. *Chlamydomonas* IFT88 is 42% identical (BLAST E = 1e − 142) to a mouse protein, called Tg737, that is required for assembly of primary cilia in the mouse kidney (Pazour et al., 2000) and node (Murcia et al., 2000). The *Caenorhabditis elegans* homologue of IFT88, OSM-5, is required for sensory cilium formation and moves within the sensory cilium (Haycraft et al., 2001; Qin et al., 2001). C*hlamydomonas* IFT57 is 38% identical (BLAST E = 3e − 67) to a mouse coiled-coil protein (unpublished data). *Chlamydomonas* IFT52 is 49% identical (BLAST E = 1e − 87) to a rodent protein called NGD5 and a *C. elegans* protein called OSM-6 (Cole et al., 1998; Deane et al., 2001). The function of NGD5 is unknown, but its expression is down-regulated by exposing cultured cells to opioids (Wick et al., 1995). OSM-6 is required for assembly of sensory cilia in nematodes (Collet et al., 1998). *Chlamydomonas* IFT20 is 32% identical (BLAST E = 4e − 15) to a small hypothetical protein in mouse as well as ESTs from humans and other vertebrate species.

IFT proteins in mouse testis and retina

Chlamydomonas IFT particles sediment as 17S complexes (Cole et al., 1998). To determine if the four mammalian homologues also are present in a large complex, we fractionated cytoplasmic extracts of mouse testis on sucrose gradients and examined the distribution of the IFT particle proteins by Western blotting (Fig. 1, a and b). Testis was chosen because the IFT proteins are much more abundant in this tissue than in any other, including retina. The four mammalian IFT proteins cosedimented at 17S, indicating that, like their algal homologues, they are part of a large complex. These data provide the first direct evidence of an IFT particle in a mammalian system and demonstrate the utility of the affinity-purified antibodies to IFT proteins.

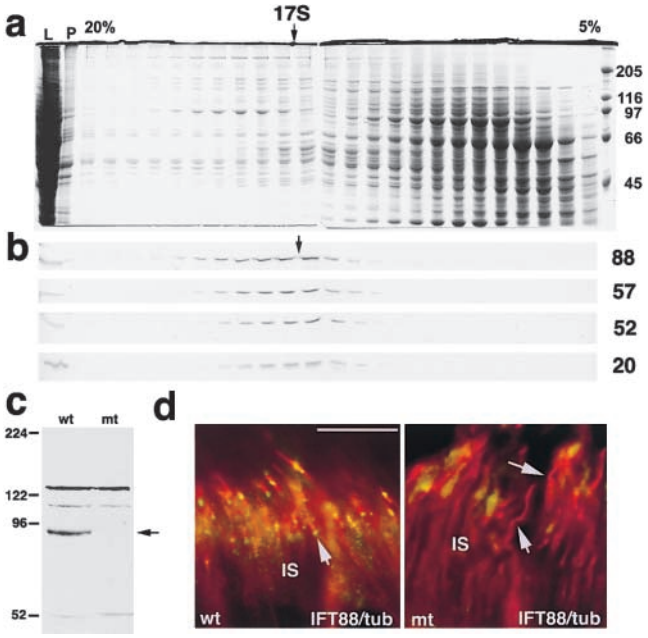

Figure 1. **IFT proteins in mouse testis and retina.** (a and b) Sucrose density gradient (5–20%) analysis of a protein extract from mouse testis showing that IFT88, IFT57, IFT52, and IFT20 cosediment at ~17S. (a) Coomasie blue–stained gels with molecular weight markers in kD indicated on right. (b) Western blots for the four IFT proteins (labeled on the right). Additional abbreviations: L, supernatant protein loaded on gradient; P, pellet from initial protein extraction. (c) Western blot of retinal extracts showing that IFT88 (arrow) is greatly reduced in $Tg737^{-/-}$ (mt) mice as compared with wild type (wt) at p21. (d) Immunofluorescence images showing that IFT88 (green) is found at the ends of the connecting cilia (red, arrows) in wild-type mouse retina but not in Tg737 mutant retina. The connecting cilia were detected by an antibody to acetylated tubulin (red). Bar, 20 μm.

IFT proteins were more difficult to detect in the retina than in the testis. Westerns of whole retinal protein extracts with the IFT88 antibody showed that wild-type retina contained an ~90-kD protein that was greatly reduced in Tg737 mutant retina (Fig. 1 c). Several additional bands were detected with this antibody. It is likely that these are unrelated cross-reactive proteins, as their level did not change in the Tg737 mutant mice. The IFT88 antibody was used to stain mutant and wild-type mouse retinas to see if differences could be detected. The IFT88 antibody (Fig. 1 d, green) strongly labeled the IS of the wild-type retina without significantly labeling this segment in the mutant. The staining was distinctly granular in nature and the brightest foci were associated with the ends of photoreceptor connecting cilia (Fig. 1 d, red). Connecting cilia could be detected in

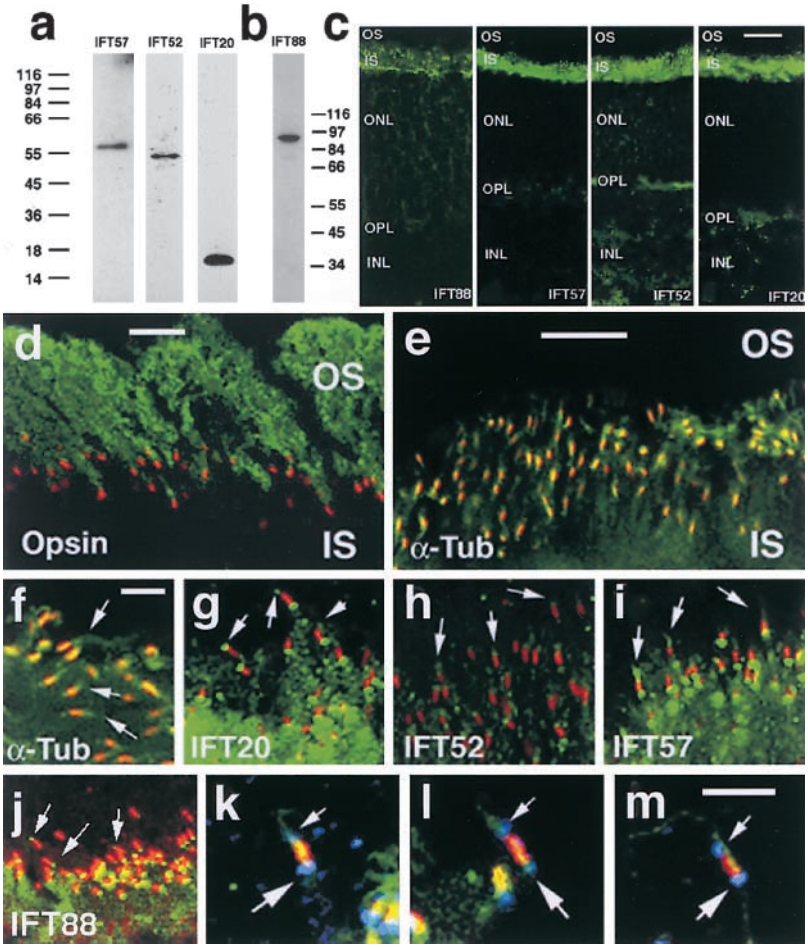

Figure 2. **IFT particle proteins are found in bovine photoreceptors.** (a and b) Western blots demonstrating the presence of IFT particle proteins in a bovine DEPC preparation that is enriched in ciliary axonemes. Antibodies raised against mouse IFT particle proteins recognize single bands of the predicted size (IFT88, 90 kD; IFT57, 57 kD; IFT52, 52 kD; IFT20, 16 kD). Numbers on left (a) and right (b) are molecular weight markers. (c) Panel of confocal immunocytochemistry images of fresh-frozen bovine retina labeled with antibodies to IFT88, IFT57, IFT52, and IFT20 from left to right. IFT particle proteins are localized primarily in the IS. Staining is punctate at the junction of the IS and OS layers where the connecting cilia are located. Staining is also detected in the outer plexiform layer (OPL), where the photoreceptor synaptic terminals are located, and to a lesser extent in the ONL. INL indicates inner nuclear layer. (d–j) Localization of IFT particle proteins to photoreceptor cilia and basal bodies. (d) Bovine OSs are labeled with the B6-30N (green) monoclonal antibody to bovine rhodopsin (Besharse and Wetzel, 1995), and connecting cilia are labeled with the K26 (red) monoclonal antibody. (e and f) Axonemes are labeled with a monoclonal antibody to acetylated α-tubulin (green), and connecting cilia are labeled with K26 (red). Arrows indicate distal ends of cilia. (g–j) Connecting cilia are detected with K26 (red), whereas IFT20 (g), IFT52 (h), IFT57 (i), and IFT88 (j) are detected with affinity-purified rabbit antibodies (green). Arrows indicate distal ends of cilia. (k–m) Triple-labeled images in which labeling with antibodies to IFT57 (blue) is superimposed over labeling of both the connecting cilium (K26, red) and acetylated α-tubulin (green). Small arrows in k–m indicate labeling that is distal to the connecting cilium; the large arrows indicate labeling that is proximal to the connecting cilium. Bars: (c) 20 μm; (d and e) 10 μm; (f) 5 μm; (m) 2 μm; (g–j) refer to e; (k and l) refer to m.

the mutant retinas but green foci were not associated with them, indicating that this staining is due to the IFT88 protein, and not one of the cross-reactive proteins.

Localization of IFT proteins to basal body and connecting cilium in bovine retina

The low abundance of IFT proteins in the retina and the small size of the mouse retina made biochemical studies difficult. To circumvent this problem, we used bovine retina. Bovine retina is often used as a biochemical system for photoreceptor research, and techniques are available for making a detergent-extracted photoreceptor cytoskeleton (DEPC) fraction that is enriched in connecting cilia (Horst et al., 1987). Furthermore, the K26 monoclonal antibody, which binds specifically to and is an excellent marker for the photoreceptor connecting cilium (Horst et al., 1990), works only in bovine photoreceptors.

Affinity-purified antibodies to IFT20, IFT52, IFT57, and IFT88 did not readily detect proteins of the expected sizes in whole cell extracts of bovine retina (unpublished data). However, these antibodies strongly detected single bands of ~16, 52, 57, and 90 kD, respectively, in the DEPC fraction (Fig. 2, a and b), suggesting that these proteins are associated with the photoreceptor connecting cilium. The retina is composed of multiple cell types, and it is likely that the failure to detect IFT proteins in whole retina is because these proteins are not abundant in the nonphotoreceptor cells. If the IFT proteins are concentrated at the connecting cilia, as the mouse result suggested, the DEPC would be greatly enriched for these proteins, as the purification of the DEPC would remove the nonphotoreceptor cells as well as most of the proteins of the photoreceptor cells.

Immunocytochemical analysis confirmed that IFT20, IFT52, IFT57, and IFT88 are most abundant in the IS of bovine photoreceptors (Fig. 2 c). The signal in the IS was distinctly granular in appearance, particularly at the boundary between the IS and OS layers where the connecting cilia are located. Much weaker immunoreactivity was also seen in the outer plexiform layer, which contains the synaptic terminals of photoreceptors. This and the presence of kinesin-II in these synapses (Muresan et al., 1999) raise the possibility that IFT proteins may have functions in photoreceptor synaptic terminals.

Double label immunocytochemistry with a monoclonal antibody (K26) that recognizes an unknown connecting cilium–specific epitope (Horst et al., 1990) demonstrated that all four IFT proteins are associated with the cilium and basal body in situ (Fig. 2, d–j). The K26 antibody uniquely stained the connecting cilia at the bases of the OSs, which were identified with antibodies to rod opsin (Fig. 2 d). In contrast, an-

tibodies to acetylated α-tubulin labeled microtubules of the IS and the ciliary axoneme (Fig. 2, e and f). Overlap of K26 (red) and acetylated α-tubulin (green) antibodies in the connecting cilium resulted in a yellow to orange color, and demonstrated that axonemal microtubules extend distally beyond the connecting cilium into the OS. Antibodies to IFT20, IFT52, IFT57, and IFT88 labeled both the proximal (IS) and distal (OS) ends of the connecting cilia in most photoreceptors (Fig. 2, g–j). Frequent yellow to orange coloration of the connecting cilium was indicative of overlap of the two labels (Fig. 2, i and j; red, K26; green, anti-IFT antibody). Triple-labeled images revealed a similar pattern (Fig. 2, k–m) in which IFT57 (blue) is associated with microtubules (green, acetylated α-tubulin) at both ends of the connecting cilium (red, K26) in most photoreceptors.

Effect of the IFT88/Tg737 mutant allele on photoreceptor cells

To directly test the role of IFT in photoreceptor cells, we examined retinas from mice homozygous for an insertional mutation in the Tg737 gene. The Tg737 allele was generated by integration of DNA into one of the exons but did not affect the coding potential of the adjacent exons. This reduces, but does not completely abolish, the ability of this gene to produce protein (Moyer et al., 1994; Taulman et al., 2001; unpublished data). Tg737 encodes IFT88 (Pazour et al., 2000), also called "polaris" (Murcia et al., 2000). Mutations in this gene cause ciliary assembly defects in *Chlamydomonas*, *C. elegans*, and the mouse kidney and embryonic node (Murcia et al., 2000; Pazour et al., 2000; Haycraft et al., 2001; Qin et al., 2001). The original Tg737 insertional mutant mouse line is homozygous for the autosomal recessive *Pdeb*^{rd1} mutation that causes rapid degeneration of photoreceptors before postnatal day (p) 20 (Carter-Dawson et al., 1978; Bowes et al., 1990; Pittler and Baehr, 1991). Because the effects of the *Pdeb*^{rd1} mutation would mask effects of the Tg737 mutation, mice were bred to eliminate one or both of the *Pdeb*^{rd1} mutant alleles. Tg737 mutant homozygotes that were both heterozygous and homozygous wild type for *Pdeb*rd were studied at p10, p21, p45, p77, and p84.

Mouse OSs normally begin to develop around p4, achieving adult proportions with well-aligned disc membranes by p20 (LaVail, 1973). In Tg737 mutant mice, a normal number of photoreceptors form, but OS structure is abnormal at all time points examined. At p10, the OSs in Tg737 mutant mice are greatly reduced in size and difficult to see by light microscopy (Fig. 3, A and B). At the EM level, the mutant OSs are disorganized. In wild-type animals, most discs are well aligned in a stacked array (Fig. 3, C and D), but this is rarely seen in Tg737 mutant OSs (Fig. 3, E and F). Instead, discs often form parallel with, rather than perpendicular to, the connecting cilium, and in some OSs the disc membranes are broken into small segments (Fig. 3 E). Another frequently seen anomaly is the development of the OS from the lateral side of the IS and partial intrusion of the OS into the IS (Fig. 3 F). This anomaly suggests breakdown of the mechanism that correctly positions the basal body, because in wild-type mice OSs always develop from the apical (distal) end of the IS.

At p21, Tg737 mutant retinas still have near normal numbers of photoreceptor nuclei in the outer nuclear layer (ONL) (Fig. 4, a–d). However, the mutant OSs are not as uniform in size or alignment and appear to be less abundant (Fig. 4, a and b). OSs of both wild type and mutant show abundant opsin immunoreactivity (Fig. 4, c and d). In contrast to wild type, opsin immunoreactivity is observed in the ISs and cell bodies of Tg737 mutant photoreceptors (Fig. 4, c and d, and Fig. 7). At the EM level (Fig. 4, e and f), the mutant photoreceptors are less uniformly aligned, less densely packed, and contain broader, less organized discs than the wild-type photoreceptors. In addi-

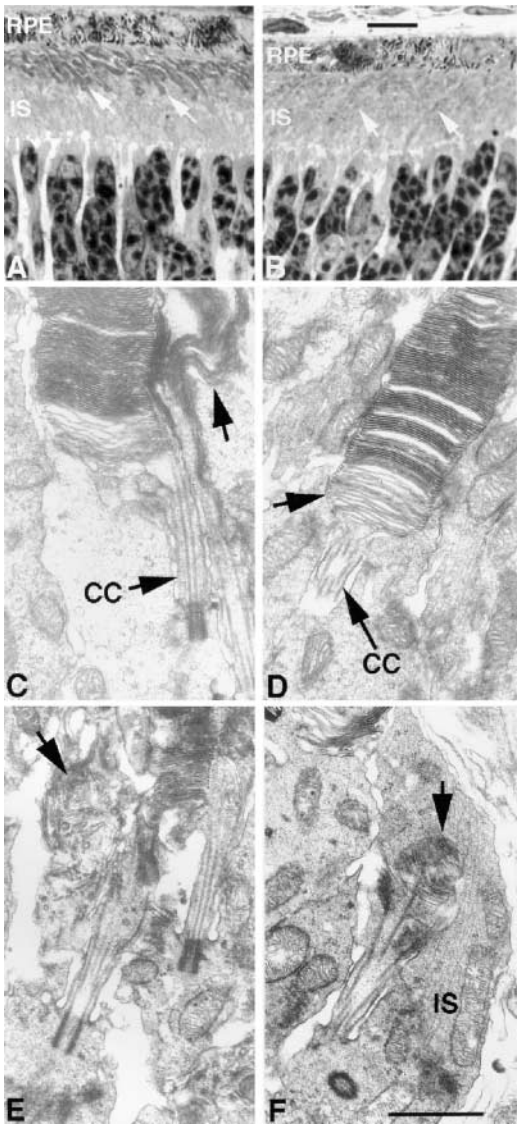

Figure 3. **Rod cell OS is abnormal in Tg737 mutant mice at p10.** (A) Typical wild-type retina showing the extent of OS development (arrows) at p10. (B) Tg737 mutant retina at p10 showing smaller and less dense OSs (arrows) than seen in wild type. RPE indicates retinal pigment epithelium. (C and D) Examples of OSs in wild-type animals at p10. In C, the arrow indicates an abnormal OS adjacent to a normal one. Such atypical OSs are only occasionally observed in wild-type mice. In D, the arrow indicates discs in the process of being formed adjacent to the connecting cilium (CC). (E and F) Typical examples of aberrant OSs in Tg737 mutant mice at p10. Disrupted discs (E, arrow) and OSs extending into their own ISs (F, arrow) are widespread in Tg737 mutant retinas at p10. Bars: (A and B) 10 μm; (C–F) 1 μm.

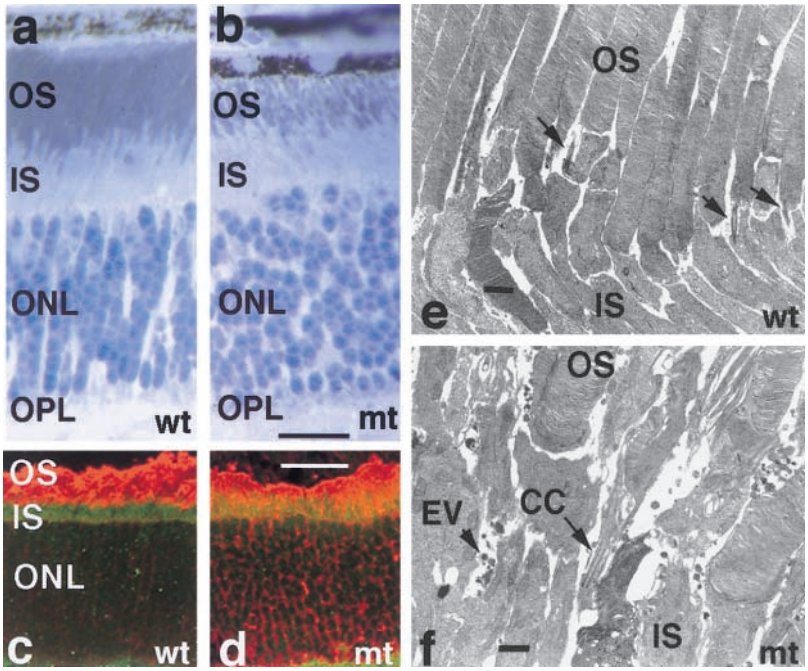

Figure 4. **Rod cell OSs are abnormal and opsin is mislocalized in Tg737 mutant mice at p21.** (a and b) Toluidine-blue–stained sections illustrating that mutant OSs (b) are less organized and less densely packed than those in similar sections of wild type (a). (c and d) Immunocytochemistry of rod opsin (red) and IFT88 (green) in frozen sections of wild-type (c) and Tg737 mutant (d) retina at p21. Both wild-type and mutant animals show strong opsin staining of the rod OS, but opsin is also detected in IS and around nuclei (ONL) in the mutant. IFT88 is present in the IS (c) but diminished in the mutant (d). (e and f) Electron micrographs of the junction between the IS and OS layers illustrating that mutant (f) photoreceptors are less uniform in structure and organization than wild-type photoreceptors (e) and accumulate extracellular vesicles (EV). Other abbreviations are the same as in figures 2 and 3. Bars: (a and b) 20 μm; (c and d) 40 μm; (e and f) 1 μm.

tion, the extracellular space of the mutant retinas is filled with vesicular material (see below).

By p45, the ONL is reduced significantly in thickness in Tg737 mutant mice compared with littermate controls (Fig. 5, A and B). Pycnotic nuclei in the mutant ONL indicate that the photoreceptor cells are dying by apoptosis. Loss of photoreceptors, measured by reduction of the ONL, reaches 60–80% (n = 6 retinas) by p77 (Fig. 5 C). In one mutant retina examined at p84, only one layer of photoreceptor nuclei could be seen (Fig. 5 D). Thus, the Tg737 mutation causes progressive photoreceptor degeneration with major loss of cells by p77. Early development of a near normal complement of photoreceptors followed by progressive loss through apoptotic cell death is characteristic of many hereditary retinal degeneration diseases in mice, but differs dramatically from the rapid degeneration before p20 seen in *Pdeb*^{rd1} mice (Carter-Dawson et al., 1978).

In the later stages of development (Fig. 6), some Tg737 mutant photoreceptors are grossly aberrant, whereas others exhibit relatively normal morphology, but even here, discs are generally significantly larger in diameter than those in wild-type photoreceptors. Although the mouse has a rod-dominant retina, the small population of cones is also disrupted (unpublished data), as would be expected if IFT88 were functioning in both photoreceptor types. In addition, retinas sampled at p21, and later, accumulate amorphous membrane vesicles in the extracellular space between cells (Fig. 6, B and D). These vesicles may be vesiculated pieces of photoreceptors that accumulate because of disrupted transport into the OS. The degenerative changes in Tg737 retinas appear to be related specifically to OSs and the death of photoreceptors. Therefore, the overall reduction in retinal thickness observed in Tg737 mutant mice can be accounted for as loss from the OS, IS, and photoreceptor nuclear layers (Fig. 5).

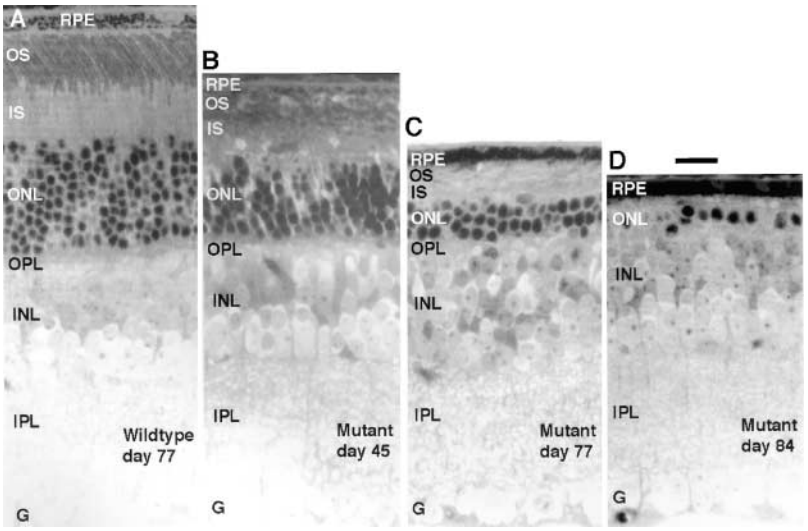

Figure 5. **Light microscopic images demonstrating progressive loss of photoreceptors in Tg737 mutant mice.** (A) Full thickness section of typical wild-type retina at p77. (B–D) Full thickness views of retinas from Tg737 mutant mice at p45, p77, and p84, showing loss of nuclei from the ONL and progressive thinning of the IS and OS layers. All images are from 1-μm-thick plastic sections stained with toluidine blue. Other abbreviations: G, ganglion cell layer; INL, inner nuclear layer; IPL, inner plexiform layer; OPL, outer plexiform layer. Bar, 20 μm.

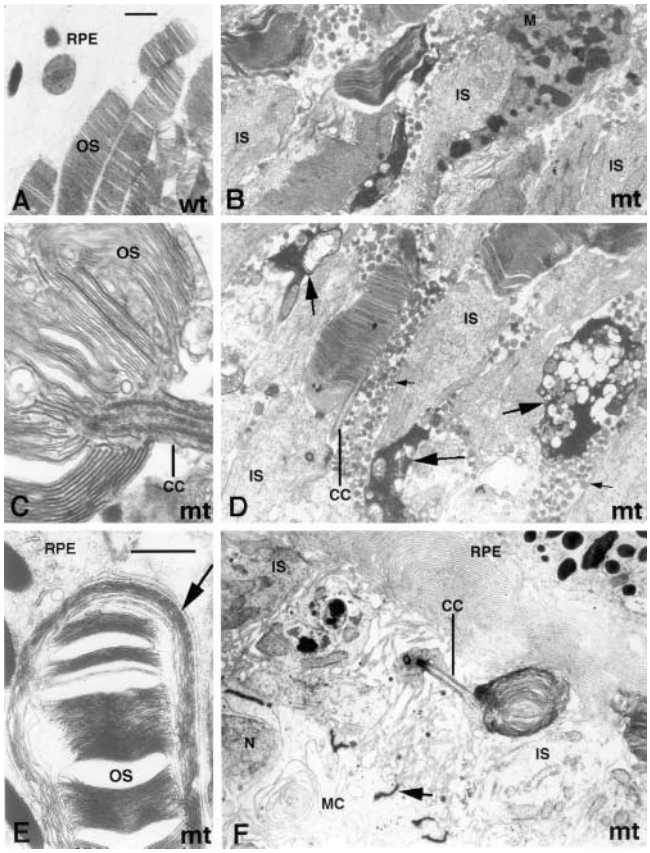

Figure 6. **EM images showing aberrant photoreceptor organization in Tg737 homozygous mutants at p45 and p77.** (A) An image of typical well-organized OSs from wild-type animals. (B–D) Tg737 mutant mice at p45. Abundant extracellular vesicles (D, small arrows) with an amorphous interior accumulate between living photoreceptors; this is never seen in wild-type animals. Condensed, dying photoreceptors are frequently seen throughout the photoreceptor layer (D, large arrows), and macrophages (B, M) are sometimes seen among photoreceptors. (E and F) Late stage of photoreceptor loss at p77. In E, a single aberrant OS adjacent to the pigment epithelium (RPE) is seen with relatively normal discs surrounded by exceptionally large disc membranes. In F, a single underdeveloped OS with whorls of disc membranes and its connecting cilium (CC) are seen adjacent to the RPE. Note that Mueller cell bodies (MC) and the junctional complexes between them (F, arrow), which normally are separated from the RPE by the full thickness of the photoreceptor IS and OS layers, are seen in the same field of view as the RPE in F. Bars: (A and E) 1 μm; (B, D, and F) refer A; (C) refer to E.

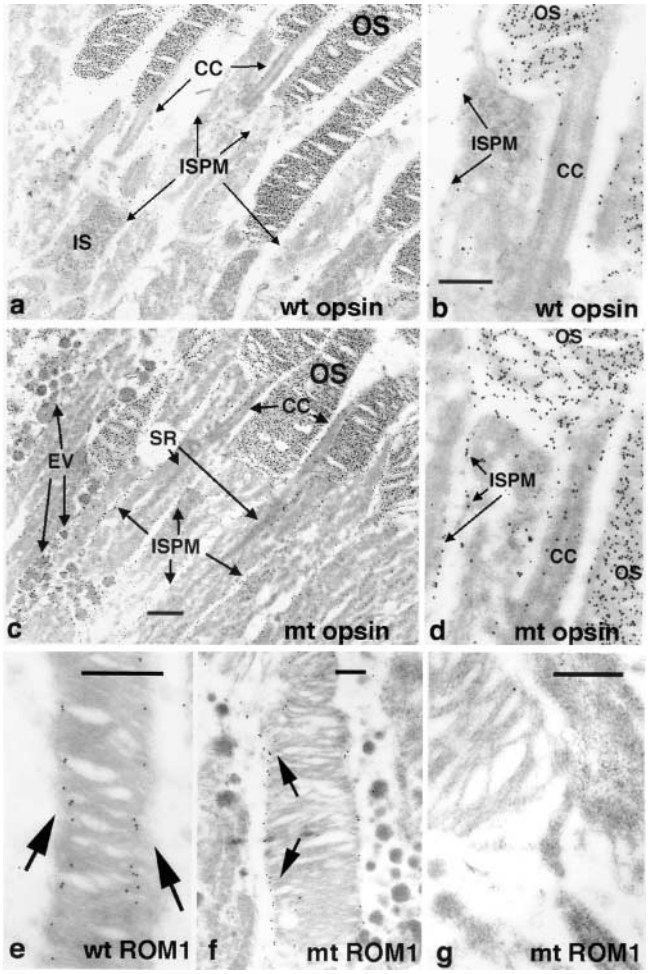

Figure 7. **EM level immunocytochemical localization of rod opsin and ROM1 in OSs of Tg737 mutant mice.** (a and b) Distribution of opsin in OSs of wild-type retinas at p21. Immunoreactivity is abundant in OSs, but very low levels are detected in the IS plasma membrane (ISPM) and connecting cilium (CC). (c and d) Distribution of opsin in OSs of Tg737 mutant retinas at p21. Opsin exhibits an abundance in mutant OSs similar to that in wild type, but is found at much higher levels compared with wild type in the IS plasma membrane and connecting cilium. In addition, opsin is present in the extracellular vesicles (EV) that are not found in wild-type animals. (e–g) Distribution of ROM1 in wild-type (e) and Tg737 (f and g) photoreceptors. ROM1 (arrows) is localized at disc edges and at incisures in wild-type animals. A similar pattern is detected in those Tg737 mutant rods that exhibit organized discs (f), but ROM1 appears to be much less abundant in OS with disorganized discs (g). Bars: (b and c) 1 μm; (e, f, and g) 0.5 μm; (a) refer to c; (d) refer to b.

Tg737 mice accumulate opsin in ISs and extracellular vesicles

Immunofluorescence microscopy (Fig. 4) indicated that the mutant photoreceptors retain opsin in their ISs and cell bodies. To more closely examine the targeting of proteins from the IS to the OS, we used postembedment immunocytochemistry. At p21 we studied the distribution of rod opsin, the most abundant OS protein, and ROM1, a protein localized in a complex with peripherin/rds at disc edges that is necessary for normal OS formation (Clarke et al., 2000). Both opsin and ROM1 are highly localized to the rod OSs in wild-type photoreceptors (Fig. 7). Opsin is found throughout the disc membrane, whereas ROM1 is associated specifically with disc edges adjacent to the OS plasma membrane. In Tg737 mutant photoreceptors, both proteins are present in OSs. However, opsin is found in much higher than normal concentrations in the connecting cilium and plasma membrane of the IS (Fig. 7, c and d). In addition, opsin (but not ROM1) is abundant in the vesicles that accumulate in the extracellular space (Fig. 7 c). ROM1 is greatly reduced or absent in mutant OSs with abnormally aligned disc membranes (Fig. 7 g), but has a relatively normal distribution in those cells with well-aligned discs (Fig. 7 f).

Discussion

IFT particle proteins and photoreceptor development

Our data provide evidence that IFT is important for normal development and maintenance of photoreceptor cells. We show that four proteins, identified by homology to components of the *Chlamydomonas* IFT particle (Cole et al., 1998), cosediment at ~17S in sucrose density gradients, consistent with their functioning as part of a mammalian IFT particle. These four proteins copurify with photoreceptor ciliary axonemes, and localize immunocytochemically to the basal body and connecting cilium of intact photoreceptors. Additional data indicate that IFT proteins are also associated with photoreceptor cilia of the fish and frog (unpublished data). The accumulation of these proteins at the basal body with lesser amounts in the ciliary axoneme is remarkably similar to the distribution of IFT particle proteins in *Chlamydomonas* (Cole et al., 1998; Pazour et al., 1999; Deane et al., 2001).

The critical importance of IFT in photoreceptors is demonstrated by our data showing that a hypomorphic mutation in the mouse Tg737/IFT88 gene leads to aberrant rod OS development and progressive photoreceptor degeneration, resulting in loss of 60–80% of the photoreceptors by p77. The basic features of the photoreceptor defect are initial aberrant, dysplastic development of both rod and cone OSs, followed by progressive photoreceptor death by apoptosis. During initial OS formation, discs fail to properly align and often are vesiculated or form parallel to the connecting cilium. Frequently, formation of the cilium occurs at sites distant from the apical region of the IS, leading to the formation of cells with anomalous polarity. Although disc rims form in many cells, discs are often unusually large, suggesting disruption of the mechanisms that normally regulate disc size. Interestingly, *rom1* mutant mice also form oversized disks (Clarke et al., 2000), and in Tg737 mutant mice, ROM1 is reduced in severely disrupted OSs. In addition to the OS structural defects, Tg737 mutant mice retain opsin in their ISs and cell bodies, and accumulate extracellular vesicles containing opsin. However, opsin trafficking is not completely disrupted as large amounts of opsin are transported to the OSs. The photoreceptor cells still alive at p77 had aberrant OSs similar to those seen early in development.

In *Chlamydomonas* and *C. elegans*, Tg737/IFT88 is absolutely required for assembly of ciliary structures (Pazour et al., 2000; Qin et al., 2001). The assembly of the connecting cilium and its development, albeit abnormal, into a rod OS in the Tg737 mutant mouse is probably made possible by the presence of a small amount of Tg737/IFT88 made from the Tg737 insertional allele. The Tg737 insertional mutation, which was generated by integration of exogenous DNA into an intron without affecting the coding potential of adjacent exons, greatly reduces but does not eliminate the production of normal-sized Tg737 message (Moyer et al., 1994) and protein (Taulman et al., 2001; unpublished data).

During the course of this work, we examined the retinas from 29 mice of various ages that were homozygous for the Tg737 mutant allele and 55 that were heterozygous or homozygous for the wild-type Tg737 allele. In all cases, the homozygous Tg737 mutant animals had abnormal photoreceptors, whereas the heterozygotes and homozygous wild-type animals had normal retinas. No differences were observed between homozygous wild-type and heterozygous mutant eyes, indicating that the Tg737 mutation is fully recessive with regard to retinal degeneration, as it is for other phenotypes (Moyer et al., 1994).

Although the original Tg737 mutant mouse also contained the *Pdeb*^{rd1} mutation, which causes retinal degeneration, the mice used in this study were the products of outcrossings that eliminated one or both copies of the *Pdeb*^{rd1} mutant allele. The retinal defects described here were not caused by the *Pdeb*^{rd1} mutation, because they were observed in mice that were homozygous for the wild-type *Pdeb* allele. Furthermore, there was no interaction between the Tg737 and *Pdeb*^{rd1} mutant alleles, because Tg737$^{-/-}$ mice on a background that was either heterozygous *Pdeb*$^{+/rd1}$ or homozygous wild type at the *Pdeb* locus had indistinguishable defects in OS formation.

Retinitis pigmentosa (RP) is a clinically and genetically heterogeneous group of retinal degeneration diseases in which photoreceptors are lost progressively through apoptotic cell death. Numerous gene mutations causing RP have been identified (http://www.sph.uth.tmc.edu/RetNet). Many of these are in retina-specific genes such as *Pdeb*rd (Bowes et al., 1990; Pittler and Baehr, 1991), opsin (Li et al., 1996), peripherin/rds (Travis et al., 1991), or ROM1 (Clarke et al., 2000). Other RP-causing mutations are in genes with broader expression patterns, such as myosin VIIA, which causes RP and deafness (Liu et al., 1999). Because IFT is important for the assembly and maintenance of all cilia and flagella, defects in IFT also would be expected to affect multiple cell types and tissues. Indeed, the Tg737 mutant mouse is defective in assembly of the primary cilia in the kidney, leading to polycystic kidney disease (Pazour et al., 2000). Thus, it is of interest that there is a longstanding connection in the literature between RP and polycystic kidney disease (see "266900 renal dysplasia and retinal aplasia" at the online Mendelian inheritance in man website, www3.ncbi.nlm.nih.gov/htbin-post/Omim/dispmim?266900). For example, both Senior-Loken and Jeune syndrome, which appear to be separate diseases, are characterized by retinal degeneration and cystic kidneys (Traboulsi et al., 1998). Tg737/IFT88 and other IFT components are likely candidates for causing these hereditary systemic disorders involving RP.

Mouse models have proved instrumental in providing insight into the mechanisms leading to degeneration, and the Tg737 mutation adds to a growing list of gene defects that appear to cause photoreceptor degeneration through disruption of pathways essential for normal assembly of the OS. Phenotypic similarities among Tg737 (this paper), pcd (Blanks and Spee, 1992), rds (Travis et al., 1991), Tulp-1$^{-/-}$ (Hagstrom et al., 1999), myosin VIIA$^{-/-}$ (Liu et al., 1999), KIF3A$^{-/-}$ (Marszalek et al., 2000), and Rom-1$^{-/-}$ (Clarke et al., 2000) mutants include formation of abnormally large discs, accumulation of extracellular vesicles, and accumulation of opsin within IS or ciliary membranes. Recently, it has been found that both overly large discs in Rom-1$^{-/-}$ mice (Clarke et al., 2000) and the accumulation of extracellular vesicles in Tulp-1$^{-/-}$ mice (Hagstrom et al.,

1999) are associated with failed OS assembly. Strikingly, we find both structural alterations in Tg737 mutant mice, arguing further that IFT provides a transport mechanism critical for normal assembly.

Model for intraphotoreceptor transport

Our data allow us to propose a model (Fig. 8) based on the idea that one or more of the cytoskeletal, membrane (including rhodopsin, peripherin-2, Rom-1, and phospholipid), or cytosolic protein components (including IFT proteins) normally synthesized in the IS and targeted to the OS via the connecting cilium are transported via IFT. The macromolecules are all synthesized in the IS. The polarity of IS microtubules (Troutt and Burnside, 1988), with their minus ends associated with the base of the cilium, suggests that membrane vesicles are transported there by cytoplasmic dynein 1. This dynein is a well-established vesicle transporter and has been shown to interact with the cytoplasmic tail of rhodopsin (Tai et al., 1999). At the base of the connecting cilium where IFT particle proteins are most concentrated, the IFT particles associate with the surface of the vesicles and components of the ciliary axoneme, as well as soluble proteins of the OS such as transducin and arrestin. Once the vesicles fuse with the plasma membrane adjacent to the cilium, the complex is moved along the connecting cilium by kinesin-II. Kinesin-II is the anterograde IFT motor in *Chlamydomonas* (Kozminski et al., 1993; Cole et al., 1998) and *Caenorhabditis* (Orozco et al., 1999; Signor et al., 1999b). Kinesin-II has been localized to the connecting cilium in vertebrates (Beech et al., 1996; Whitehead et al., 1999), and mice with photoreceptor-specific defects in the KIF3A subunit of kinesin-II accumulate opsin and arrestin in the IS (Marszalek et al., 2000). In the OS, the IFT particles disengage from their cargo, and the membrane is organized into disks through a mechanism involving myosin VIIA. Myosin VII is required for phagocytosis in *Dictyostelium* (Titus, 1999), and mice with defects in the myosin VIIA gene accumulate opsin in the connecting cilium (Liu et al., 1999). Soluble proteins of the transduction machinery and cytoskeleton then associate with appropriate protein complexes within the OS, and IFT particles that have reached the distal end of the connecting cilium are returned to the base of the cilium by cytoplasmic dynein 1b/2. This dynein is the retrograde IFT motor in *Chlamydomonas* (Pazour et al., 1998, 1999; Porter et al., 1999) and *Caenorhabditis* (Signor et al., 1999a) and has been localized to the connecting cilium of vertebrate photoreceptors (unpublished data). At the base of the connecting cilium, the IFT particles reenter a peribasal body pool of IFT particle proteins and begin the cycle again. The IFT particles also may move components of the transduction machinery from the OS to the IS. For example, both transducin and arrestin have been reported to rapidly move between the segments during light and dark adaptation (Philp et al., 1987; Whelan and McGinnis, 1988), and arrestin accumulates in the IS in KIF3A mutant mice (Marszalek et al., 2000).

Comparison to kinesin-II Cre-Lox mice

The recent finding (Marszalek et al., 2000) that a conditional knockout of the KIF3A subunit of kinesin-II in mouse photoreceptors results in photoreceptor degeneration

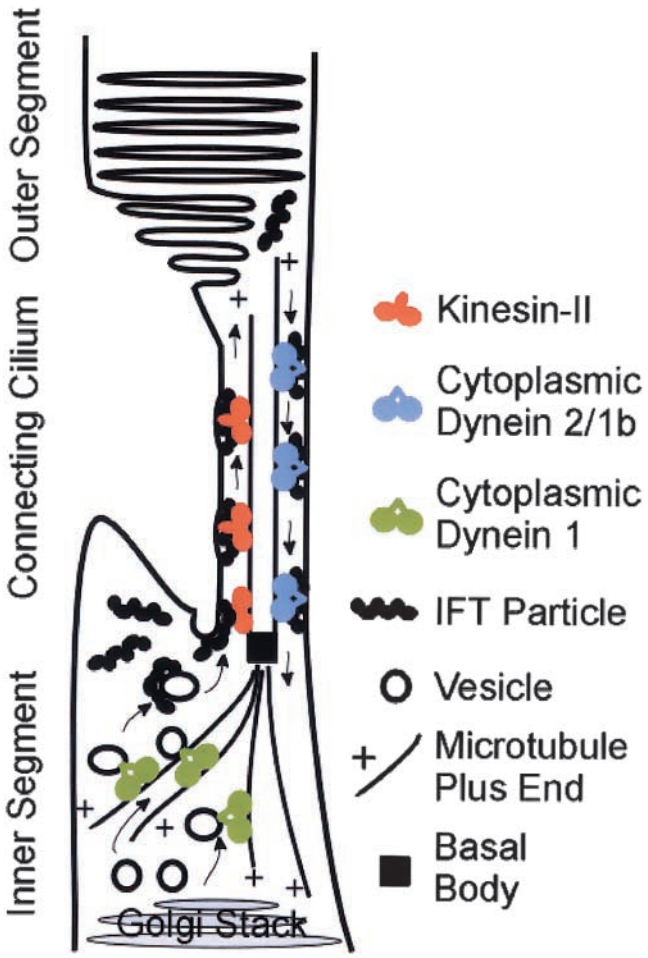

Figure 8. **Model of photoreceptor cell IFT.** Cytoplasmic dynein 1 transports vesicles from the Golgi stack to the base of the connecting cilium. IFT particles associate with the vesicles and the vesicles fuse with the ciliary or plasma membrane at the base of the connecting cilium. The IFT particles with attached cargo are then transported through the connecting cilium by kinesin-II. At the distal end of the connecting cilium, the IFT particles dissociate from their cargo, the membrane is organized into disks, and the IFT particles are picked up by cytoplasmic dynein 1b/2 to be returned to the cell body.

is similar to our findings for the Tg737 mutation. Both mutations cause accumulation of opsin in the IS and result in substantial age-related loss of photoreceptors. The principal difference in the two phenotypes is that kinesin-II mutant mice accumulate intracellular vesicles in the IS before degeneration of affected cells, whereas Tg737 mutant mice accumulate extracellular vesicles and show anomalous OS development before degeneration. Although the initial IS defect in the KIF3A mutant mice may reflect a nonciliary role for kinesin-II in photoreceptors, it seems likely that the principal differences between the two relates to the fact that the kinesin-II defect appears suddenly in individual cells after the OSs have developed (Marszalek et al., 2000), whereas the hypomorphic Tg737 mice have an insufficient quantity of IFT88 during development and do not form proper OSs. In both the Tg737 and the kinesin-II mutant mice, opsin accumulates within the IS, and it has been suggested that kinesin-II specifically transports opsin (Marszalek et al., 2000).

Although opsin is a potential cargo for IFT, its accumulation in IS membranes is a general feature of diverse photoreceptor degenerations (Nir and Papermaster, 1986; Nir et al., 1987; Hagstrom et al., 1999) and could result indirectly from multiple defects that alter the transport/assembly of discs in the OS. Current work directed at identifying proteins that interact with IFT particles may provide insight into the specific cargo delivered through IFT.

Materials and methods

Cloning IFT20

Chlamydomonas IFT20 was purified, and the sequences of two tryptic peptides (GVYFDEDFHVR and YVSAIDQQVER) were obtained (Cole et al., 1998). A degenerate PCR primer designed from the first peptide sequence was used in combination with an oligo-dT primer to amplify most of the coding sequence from reverse-transcribed cDNA. The remainder of the gene was amplified from a *Chlamydomonas* cDNA library in lambda ZapII (Stratagene) with a vector primer (M13Rev) and a IFT20-specific primer designed from the sequence of the first PCR product. The open reading frame contained within these clones encodes a 15.6-kD peptide containing both tryptic peptides.

Antibody production

The antibodies were produced in rabbits by injecting bacterially expressed maltose-binding fusion proteins made by cloning the entire open reading frames of mouse NDG5 (IFT52), IFT57, and IFT20, and the COOH-terminal 459 codons of Tg737 (IFT88) into the pMalc expression vector (New England Biolabs, Inc.). The sera were affinity purified using immobilized glutathione-*S*-transferase fusion proteins. The latter fusion proteins were made by cloning the open reading frames of the IFT genes into the pGEX-6p-1 (Amersham Pharmacia Biotech) expression vector.

Preparation of the DEPC and Western blotting

Whole retinal extracts of mouse and bovine retina were prepared by direct solublization in SDS sample buffer. The DEPC was prepared as described by Horst et al. (1987). In brief, rod OSs shaken from 50 dark-adapted, frozen bovine retinas in buffer A (10 mM Pipes, pH 7.0, 1 mM EDTA, 5 mM $MgCl_2$, 0.02% NaN_3), supplemented with a protease inhibitor cocktail (1 μg/ml pepstatin, 1 μg/ml leupeptin, 4 μg/ml aprotinin, 1 mM benzamidine, 1 mM PMSF), were purified by sucrose density centrifugation. OSs were then extracted in buffer A containing 2% Triton X-100. Ciliary axonemes were separated from detergent-soluble material by centrifugation over a 45–60% linear sucrose gradient. Equal aliquots were separated on a 12% denaturing polyacrylamide gel and transferred to Immobilon™ membranes for antibody labeling and detection using the SuperSignal West Femto chemiluminescent system (Pierce Chemical Co.). The Western blot analysis of mutant mouse retinal tissue with IFT88 antibodies was conducted on homozygous mutant and wild-type mice at p21.

Sucrose gradient analysis

Sucrose density gradient analysis was performed according to the procedures of Cole et al. (1998) using five frozen mouse testes (0.5 g of tissue; Pel-Freez Biologicals). Tissue was thawed, diced, and homogenized for 2 min in a Dounce homogenizer in 0.5 ml of HMDEK buffer (Cole et al., 1998) containing protease inhibitors: 2.5 mM 4-aminobenzamidine, 2.0 mM PMSF, 1 μg/ml pepstatin A, 1 μg/ml aprotinin, 1 μg/ml leupeptin, and 50 μg/ml soybean trypsin inhibitor. After 10 min on ice, the homogenate was centrifuged (16,000 *g*) for 10 min at 4°C, and the supernatant was further centrifuged (178,000 *g*; Beckman Airfuge) for 5 min at 25°C. NaCl was added to a final concentration of 300 mM and the supernatant was fractionated on a 5–20% linear sucrose gradient containing 300 mM NaCl in HMDEK.

Immunofluorescence and confocal imaging

Fresh mouse or bovine retinal tissue was placed in Tissue Freezing Medium™ (Triangle Biomedical Sciences) and quickly frozen in liquid nitrogen with or without prior fixation in 4% paraformaldehyde. For the immunofluorescence of mouse retina in Fig. 1, fixed tissue was embedded in paraffin. After removal of the paraffin, the sections were boiled for 10 min in 10 mM sodium citrate (pH 6) and treated with 0.1% sodium borohydride in PBS for 30 min. For the immunofluorescence of mouse retina in Fig. 4, frozen sections were boiled for 15 min in 10 mM sodium citrate buffer. Primary antibodies were detected with goat anti–rabbit or goat anti–mouse IgG conjugated with Cy3 (Jackson ImmunoResearch Laboratories), Texas red™, fluorescein, Alexa 488, Alexa 568, or Alexa 633 (Molecular Probes). In double label experiments, discrimination of signals for K26 versus IFT proteins involved the use of conjugated anti–mouse and anti–rabbit antibodies, respectively. For discrimination of two monoclonal antibodies (K26 vs. tubulin or opsin), we labeled with one monoclonal antibody and a fluorescent anti–mouse antibody, and then repeated the procedure for the second monoclonal antibody using a different fluorophore. Images of cells labeled with more than one fluorophore were pseudocolored and merged using NIH Image 1.62 or Adobe Photoshop®. Antibodies used in these studies were the four IFT antibodies (above), an antirhodopsin monoclonal antibody (B630N; Besharse and Wetzel, 1995), a monoclonal anti-acetylated α-tubulin antibody (611β1; Sigma-Aldrich), an antibody to ROM1 (provided by Rod McInnes, University of Toronto, Toronto, Canada), and a monoclonal antibody (K26) directed at an unidentified epitope of the bovine photoreceptor connecting cilium (Horst et al., 1990).

Mouse breeding

The original TgN737Rpw mouse line was homozygous for the autosomal recessive *Pdeb*^{rd1} retinal degeneration defect, precluding analysis of the effect of the Tg737 mutation on retinal development. To produce animals suitable for analysis, heterozygous Tg737 mutant mice on the FVB/N (*+/TgN737Rpw, Pdeb*^{rd1}/Pdeb^{rd1}) background were bred to wild-type C57B6/J (+/+, +/+) animals, and the offspring from this cross were sibling mated to produce F2 animals, or backcrossed to the heterozygous Tg737 FVB/N parent. The Tg737 mutation was genotyped as described by Pazour et al. (2000). *Pdeb*^{rd1} was genotyped using a Dde1 restriction site polymorphism (Pittler and Baehr, 1991) that results from the *Pdeb*^{rd1} mutation.

EM

For conventional EM, eyes of Tg737 mutant animals and littermate controls were removed at p10, p21, p45, and p77. At least six Tg737$^{-/-}$ mutant eyes and Tg737$^{+/+}$ controls were analyzed at each time; one additional mutant was examined at p84. After making an incision in the cornea on the dorsal side, eyes were fixed by immersion in 2.5% glutaraldehyde and 2% formaldehyde in phosphate buffer for 1–2 d. The cornea, iris, and lens were then surgically removed and the eye cups were postfixed in 1% osmium tetroxide for 2 h, dehydrated in ethanol, and embedded in Embed 812 (Electron Microscopy Sciences). At the time of embedment, eyes were oriented so that sections could be obtained parallel to the dorsoventral meridian. 1-μm-thick sections were stained with toluidine blue, and silver-gold thin sections were stained with uranyl acetate and lead citrate after conventional procedures**.** All analyses were conducted on cells in the central retina (posterior pole) in sections through the dorsoventral meridian.

Postembedment EM immunocytochemistry

For postembedment EM immunocytochemistry, eyes from Tg737 mutant animals and littermate controls at p21 were removed and fixed in 4% paraformaldehyde in phosphate buffer for 1–2 d. They were then dehydrated in ethanol and embedded in LR White medium (Polysciences) as described previously (Besharse and Wetzel, 1995). Thin sections were then incubated with a monoclonal antibody (B6-30N) directed at the NH_2 terminus of rod opsin (Besharse and Wetzel, 1995) or with affinity-purified rabbit antibodies directed against the COOH terminus of ROM-1 (Clarke et al., 2000). Primary antibodies were detected with anti–mouse or anti–rabbit IgG conjugated with 10 nm colloidal gold (Amersham Pharmacia Biotech). Sections were subsequently stained with uranyl acetate for 7 min at 60°C to enhance contrast.

Toluidine blue–stained sections were imaged using a CoolSnap video camera mounted on a Nikon Eclipse TE300 inverted microscope. The resulting digital images were archived at 72 pixels per inch. Standard EM prints at 5,000 to 20,000 magnification were scanned for conversion to digital images and archived without further processing at 200 pixels per inch. Composite images were arranged using Adobe Photoshop®; image processing was limited to adjustments of brightness and contrast.

GenBank/EMBL/DDBJ accession nos.

IFT20: *Chlamydomonas* (accession no. AF285762), *Xenopus* (AY048114), chicken (BG711517), pig (BF075374), cattle (AV597208), rat (AI170881), mouse (AAA81518, AY082613), and human (AA099304). IFT88: mouse (NP033042). IFT52: mouse (AAA96241).

The authors thank Wolfgang Baehr (Moran Eye Center, Salt Lake City, UT) and Dennis Diener (Yale University, New Haven, CT) for helpful discussions, Rod McInnes for the ROM-1 antibody, and Scott Seeley and Marleen Janson for technical support. We also thank Greg Hendricks from the University of Massachusetts Medical School (UMMS) EM facility, Greg Ning from the Medical College of Wisconsin (MCW) EM facility, and Anna

Fekete from the MCW Ophthalmology facility for technical support.

This work was supported by grants from the National Institutes of Health (GM-60992 to G.J. Pazour; GM-30626 to G.B. Witman; GM-14642 to J.L. Rosenbaum; EY-03222 to J.C. Besharse), by a National Eye Institute core grant for Vision Research (EY01931 to J.C. Besharse), by a Diabetes and Endocrinology Research Center grant (DK 32520) at UMMS, and by the Robert W. Booth Fund at the Greater Worcester Community Foundation (G.B. Witman).

Submitted: 26 July 2001
Revised: 14 February 2002
Accepted: 15 February 2002

References

Anderson, R.E., M.B. Maude, P.A. Kelleher, T.M. Maida, and S.F. Basinger. 1980. Metabolism of phosphatidylcholine in the frog retina. *Biochim. Biophys. Acta.* 620:212–226.

Beech, P.L., K. Pagh-Roehl, Y. Noda, N. Hirokawa, B. Burnside, and J.L. Rosenbaum. 1996. Localization of kinesin superfamily proteins to the connecting cilium of fish photoreceptors. *J. Cell Sci.* 109:889–897.

Besharse, J.C., and C.J. Horst. 1990. The photoreceptor connecting cilium. A model for the transition zone. *In* Ciliary and Flagellar Membranes. R.A. Bloodgood, editor. Plenum Publishing Corp, New York. 389–417.

Besharse, J.C., and M.G. Wetzel. 1995. Immunocytochemical localization of opsin in rod photoreceptors during periods of rapid disc assembly. *J. Neurocytol.* 24:371–388.

Blanks, J.C., and C. Spee. 1992. Retinal degeneration in the pcd/pcd mutant mouse: accumulation of spherules in the interphotoreceptor space. *Exp. Eye Res.* 54:637–644.

Bowes, C., T. Li, M. Danciger, L.C. Baxter, M.L. Applebury, and D.B. Farber. 1990. Retinal degeneration in the rd mouse is caused by a defect in the β subunit of rod cGMP-phosphodiesterase. *Nature*. 347:677–680.

Carter-Dawson, L.D., M.M. LaVail, and R.L. Sidman. 1978. Differential effect of the rd mutation on rods and cones in the mouse retina. *Invest. Ophthalmol. Vis. Sci.* 17:489–498.

Clarke, G., A.F.X. Goldberg, D. Vidgen, L. Collins, L. Ploder, L. Schwarz, L.L. Molday, J. Rossant, A. Szél, R.S. Molday, et al. 2000. Rom-1 is required for rod photoreceptor viability and the regulation of disk morphogenesis. *Nat. Genet.* 25:67–73.

Cole, D.G., D.R. Diener, A.L. Himelblau, P.L. Beech, J.C. Fuster, and J.L. Rosenbaum. 1998. *Chlamydomonas* kinesin-II–dependent intraflagellar transport (IFT): IFT particles contain proteins required for ciliary assembly in *Caenorhabditis elegans* sensory neurons. *J. Cell Biol.* 141:993–1008.

Collet, J., C.A. Spike, J.E. Lundquist, J.E. Shaw, and R.K. Herman. 1998. Analysis of osm-6, a gene that affects sensory cilium structure and sensory neuron function in *Caenorhabditis elegans. Genetics.* 148:187–200.

Deane, J.A., D.G. Cole, E.S. Seeley, D.R. Diener, and J.L. Rosenbaum. 2001. Localization of intraflagellar transport protein IFT52 identifies the transition fibers of the basal body as the docking site for IFT particles. *Curr. Biol.* 11: 1586–1590.

Hagstrom, S.A., M. Duyao, M.A. North, and T.S. Li. 1999. Retinal degeneration in *tulp1*$^{-/-}$ mice: vesicular accumulation in the interphotoreceptor matrix. *Invest. Ophthalmol. Vis. Sci.* 40:2795–2802.

Haycraft, C.J., P. Swoboda, P.D. Taulman, J.H. Thomas, and B.K. Yoder. 2001. The *C. elegans* homolog of the murine cystic kidney disease gene Tg737 functions in a ciliogenic pathway and is disrupted in osm-5 mutant worms. *Development.* 128:1493–1505.

Horst, C.J., D.M. Forestner, and J.C. Besharse. 1987. Cytoskeletal–membrane interactions: a stable interaction between cell surface glycoconjugates and doublet microtubules of the photoreceptor connecting cilium. *J. Cell Biol.* 105: 2973–2987.

Horst, C.J., L.V. Johnson, and J.C. Besharse. 1990. Transmembrane assemblage of the photoreceptor connecting cilium and motile cilium transition zone contain a common immunologic epitope. *Cell Motil. Cytoskeleton.* 17:329–344.

Kozminski, K.G., K.A. Johnson, P. Forscher, and J.L. Rosenbaum. 1993. A motility in the eukaryotic flagellum unrelated to flagellar beating. *Proc. Natl. Acad. Sci. USA.* 90:5519–5523.

LaVail, M.M. 1973. Kinetics of rod outer segment renewal in the developing mouse retina. *J. Cell Biol.* 58:650–661.

Li, T., W.K. Snyder, J.E. Olsson, and T.P. Dryja. 1996. Transgenic mice carrying the dominant rhodopsin mutation P347S: evidence for defective vectorial transport of rhodopsin to the outer segments. *Proc. Natl. Acad. Sci. USA.* 93: 14176–14181.

Liu, X.R., I.P. Udovichenko, S.D.M. Brown, K.P. Steel, and D.S. Williams. 1999. Myosin VIIa participates in opsin transport through the photoreceptor cilium. *J. Neurosci.* 19:6267–6274.

Marszalek, J.R., and L.S.B. Goldstein. 2000. Understanding the functions of kinesin-II. *Biochim. Biophys. Acta.* 1496:142–150.

Marszalek, J.R., X.R. Liu, E.A. Roberts, D. Chui, J.D. Marth, D.S. Williams, and L.S.B. Goldstein. 2000. Genetic evidence for selective transport of opsin and arrestin by kinesin-II in mammalian photoreceptors. *Cell.* 102:175–187.

Morris, R.L., and J.M. Scholey. 1997. Heterotrimeric kinesin-II is required for the assembly of motile 9+2 ciliary axonemes on sea urchin embryos. *J. Cell Biol.* 138:1009–1022.

Moyer, J.H., M.J. Lee-Tischler, H.-Y. Kwon, J.J. Schrick, E.D. Avner, W.E. Sweeney, V.L. Godfrey, N.L. Cacheiro, J.E. Wilkinson, and R.P. Woychik. 1994. Candidate gene associated with a mutation causing recessive polycystic kidney disease in mice. *Science.* 264:1329–1333.

Murcia, N.S., W.G. Richards, B.K. Yoder, M.L. Mucenski, J.R. Dunlap, and R.P. Woychik. 2000. The *Oak Ridge Polycystic Kidney* (*orpk*) disease gene is required for left-right axis determination. *Development.* 127:2347–2355.

Muresan, V., A. Lyass, and B.J. Schnapp. 1999. The kinesin motor KIF3A is a component of the presynaptic ribbon in vertebrate photoreceptors. *J. Neurosci.* 19:1027–1037.

Nir, I., and D.S. Papermaster. 1986. Immunocytochemical localization of opsin in the inner segment and ciliary plasma membrane of photoreceptors in retinas of rds mutant mice. *Invest. Ophthalmol. Vis. Sci.* 27:836–840.

Nir, I., G. Sagie, and D.S. Papermaster. 1987. Opsin accumulation in photoreceptor inner segment plasma membranes of dystrophic RCS rats. *Invest. Ophthalmol. Vis. Sci.* 28:62–69.

Orozco, J.T., K.P. Wedaman, D. Signor, S. Brown, L. Rose, and J.M. Scholey. 1999. Movement of motor and cargo along cilia. *Nature.* 398:674.

Pazour, G.J., C.G. Wilkerson, and G.B. Witman. 1998. A dynein light chain is essential for the retrograde particle movement of intraflagellar transport (IFT). *J. Cell Biol.* 141:979–992.

Pazour, G.J., B.L. Dickert, and G.B. Witman. 1999. The DHC1b (DHC2) isoform of cytoplasmic dynein is required for flagellar assembly. *J. Cell Biol.* 144:473–481.

Pazour, G.J., B.L. Dickert, Y. Vucica, E.S. Seeley, J.L. Rosenbaum, G.B. Witman, and D.G. Cole. 2000. *Chlamydomonas* IFT88 and its mouse homologue, polycystic kidney disease gene *Tg737*, are required for assembly of cilia and flagella. *J. Cell Biol.* 151:709–718.

Philp, N.J., W. Chang, and K. Long. 1987. Light-stimulated protein movement in rod photoreceptor cells of the rat retina. *FEBS Lett.* 225:127–132.

Piperno, G., and K. Mead. 1997. Transport of a novel complex in the cytoplasmic matrix of *Chlamydomonas* flagella. *Proc. Natl. Acad. Sci. USA.* 94:4457–4462.

Pittler, S.J., and W. Baehr. 1991. Identification of a nonsense mutation in the rod photoreceptor cGMP phosphodiesterase β-subunit gene of the *rd* mouse. *Proc. Natl. Acad. Sci. USA.* 88:8322–8326.

Porter, M.E., R. Bower, J.A. Knott, P. Byrd, and W. Dentler. 1999. Cytoplasmic dynein heavy chain 1b is required for flagellar assembly in *Chlamydomonas. Mol. Biol. Cell.* 10:693–712.

Qin, H., J.L. Rosenbaum, and M.M. Barr. 2001. An autosomal recessive polycystic kidney disease gene homolog is involved in intraflagellar transport in *C. elegans* ciliated sensory neurons. *Curr. Biol.* 11:457–461.

Rosenbaum, J.L., D.G. Cole, and D.R. Diener. 1999. Intraflagellar transport: the eyes have it. *J. Cell Biol.* 144:385–388.

Signor, D., K.P. Wedaman, J.T. Orozco, N.D. Dwyer, C.I. Bargmann, L.S. Rose, and J.M. Scholey. 1999a. Role of a class DHC1b dynein in retrograde transport of IFT motors and IFT raft particles along cilia, but not dendrites, in chemosensory neurons of living *Caenorhabditis elegans. J. Cell Biol.* 147: 519–530.

Signor, D., K.P. Wedaman, L.S. Rose, and J.M. Scholey. 1999b. Two heteromeric kinesin complexes in chemosensory neurons and sensory cilia of *Caenorhabditis elegans. Mol. Biol. Cell.* 10:345–360.

Tai, A.W., J.Z. Chuang, C. Bode, U. Wolfrum, and C.H. Sung. 1999. Rhodopsin's carboxy-terminal cytoplasmic tail acts as a membrane receptor for cytoplasmic dynein by binding to the dynein light chain Tctex-1. *Cell.* 97:877–887.

Taulman, P.D., C.J. Haycraft, D.F. Balkovetz, and B.K. Yoder. 2001. Polaris, a protein involved in left-right axis patterning, localizes to basal bodies and cilia. *Mol. Biol. Cell.* 12:589–599.

Titus, M.A., 1999. A class VII unconventional myosin is required for phagocytosis. *Curr. Biol.* 9:1297–1303.

Traboulsi, E.I., A.V. Drack, and H. Salama. 1998. Pigmentary retinopathy and systemic disease. *In* Genetic Diseases of the Eye. E.I. Traboulsi, editor. Oxford University Press, New York. 629–662.

Travis, G.H., J. Gregor Sutcliffe, and D. Bok. 1991. The retinal degeneration slow (rds) gene product is a photoreceptor disc membrane-associated glycoprotein. *Neuron.* 6:61–70.

Troutt, L.L., and B. Burnside. 1988. Microtubule polarity and distribution in teleost photoreceptors. *J. Neurosci.* 8:2371–2380.

Whelan, J.P., and J.F. McGinnis. 1988. Light-dependent subcellular movement of photoreceptor proteins. *J. Neurosci. Res.* 20:263–270.

Whitehead, J.L., S.Y. Wang, L. Bost-Usinger, E. Hoang, K.A. Frazer, and B. Burnside. 1999. Photoreceptor localization of the KIF3A and KIF3B subunits of the heterotrimeric microtubule motor kinesin II in vertebrate retina. *Exp. Eye Res.* 69:491–503.

Wick, M.J., D.K. Ann, and H.H. Loh. 1995. Molecular cloning of a novel protein regulated by opioid treatment of NG108-15 cells. *Brain Res. Mol. Brain Res.* 32:171–175.

Young, R.W. 1967. The renewal of photoreceptor cell outer segments. *J. Cell Biol.* 33:61–72.